# Fusion and Fragmentation Dynamics at Equilibrium in Triblock Copolymer Micelles

**ARTICLE** *in* MACROMOLECULES · DECEMBER 2012

Impact Factor: 5.8 · DOI: 10.1021/ma3018298



**1 AUTHOR:**

Yahya Rharbi

French National Centre for Scientific Research

**60** PUBLICATIONS **1,094** CITATIONS

Macromolecules

Article

pubs.acs.org/Macromolecules

# Fusion and Fragmentation Dynamics at Equilibrium in Triblock Copolymer Micelles

Y. Rharbi*

Laboratoire de Rhéologie et procédés, CNRS/UJF/INPG, UMR 5520, B.P.53, F-38041 Grenoble Cedex 9, France

**ABSTRACT:** Amphiphilic block copolymers autoassemble in water to form either dynamically active micelles or frozen particles at high surface tension. The dynamics of these systems is dominated by an individual process, which involves insertion−expulsion of copolymer chains, and a collective one, which involves fusion and fragmentation of proper micelles. The details of these mechanisms can drastically affect the micelles' morphology and some of their applications (drug delivery, template for mesoscopic structures, etc.). While fusion and fragmentation were found to be important in out-of-equilibrium kinetics such as sphere-to-rod transition, they were reported to be irrelevant at equilibrium by both theories and chain randomization experiments. We show, for the first time, that fusion and fragmentation do in fact take place at equilibrium in triblock copolymer micelles poly(ethylene oxide)−poly(propylene oxide)−poly(ethylene oxide). This was achieved using a fluorescent technique, which probes the randomization of hydrophobic pyrene derivatives between micelles.

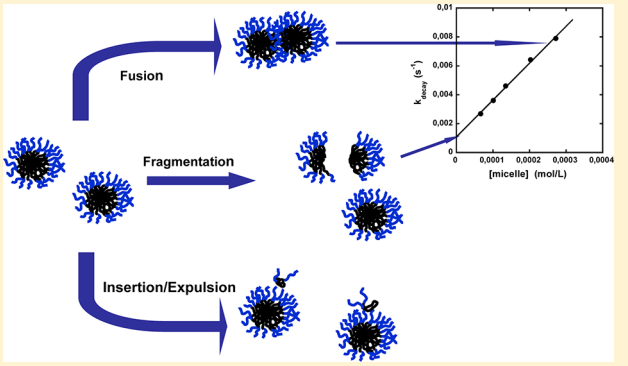


When amphiphilic block copolymers are dissolved in aqueous solution, they form micelle aggregates with the hydrophobic block in the core and the hydrophilic part in the corona.[1] Unlike small surfactants, which are dynamically active, block copolymers exhibit slow to frozen kinetics.[2] Particularly when the surface tension between blocks is high, they can be trapped in metastable states without reaching their thermodynamic equilibrium.[2] The kinetic in surfactant micelles is dominated by two mechanisms.[3,4] The first, described by Anniasson and Wall (A−W), involves unimer/micelle interactions via insertion−expulsion of unimers.[3] The second involves micelle−micelle interactions via fusion and fragmentation.[5,6] Yet, the dynamics in block copolymer micelles differs from the surfactant kinetics due to the chain correlation in the core and the strong steric repulsion of the corona.[2b]

Halperin and Alexander predicted insertion−expulsion to be the main dynamic process in diblock copolymers (Chart 1, path d),[7] whereas Dormidonto argued that fusion and fragmentation (Chart 1, paths b and c) are favorable in the early stage of micellization while unimer insertion−expulsion is the main process at equilibrium.[8] Kinetic experiments at equilibrium involving randomization of diblock copolymers between micelles shows that insertion−expulsion is the main path for the chain exchange.[2b] Fusion and fragmentation of block copolymer micelles were observed in experiments involving morphological transition such as spheres-to-rod-like micelles.[9−11] Yet, to our knowledge there are no reports on the fusion and fragmentation at equilibrium in block copolymers.

In this work, we monitor the fusion and fragmentation dynamic at equilibrium in the triblock copolymer poly(ethylene oxide)−poly(propylene oxide)−poly(ethylene oxide) with relatively large molecular weights ($PEO_{17}PPO_{60}PEO_{17}$). We use a fluorescent technique that was discovered few years ago by some of the authors of this paper, which exploits the randomization of hydrophobic pyrene derivatives ($PyC_{18}$) between micelles as a tool to probe the fusion and fragmentation.[6] We show that fusion−fragmentation and

**Chart 1. Various Processes for Exchanging the Copolymer Chains and Probes (P) between Micelles: (a) Exit−Entry of the Probe, (b) Fragmentation−Growth, (c) Fusion−Fragmentation, and (d) Insertion−Expulsion of Individual Chain**

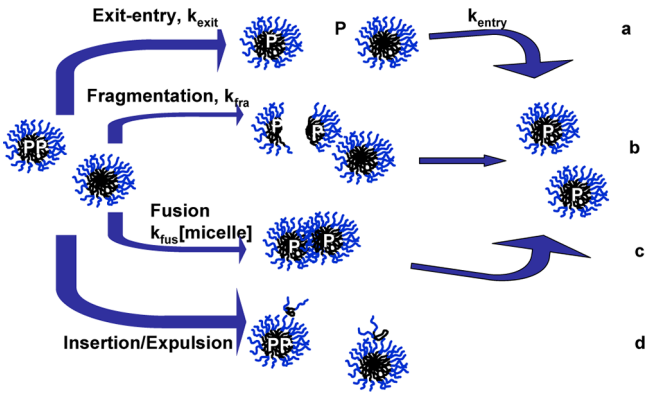


**Received:** September 5, 2012
**Revised:** October 9, 2012

   dx.doi.org/10.1021/ma3018298 | *Macromolecules* XXXX, XXX, XXX−XXX

fragmentation−growth take place in the triblock copolymer P103 micelle with very slow rates.

Triblock copolymer Pluronic P103 ($PEO_{17}PPO_{60}PEO_{17}$) with $M_w$ = 4.95 kg/mol (BASF Corp.) was used as received. Doubly deionized water was used in the preparation of the P103 solutions. The probe 1-pyrenyloctadecanone, $C_{34}H_{44}O$ ($PyC_{18}$), was prepared via a Friedel−Crafts acylation of pyrene with stearoyl chloride in dichloroethane and in the presence of aluminum chloride ($AlCl_3$).[12] The $PyC_{18}$ was solubilized in P103 micelles by mixing P103 (20 g/L) with traces of $PyC_{18}$ at 85 °C. The solution was strongly agitated for 10 min with a Vortex genie 2 model G 650 mechanical shaker at its maximum frequency (>10 Hz). The solution was centrifuged at 5000 rpm for 15 min at 25 °C to remove the nondissolved probe. Fluorescence measurements were carried out with a Fluorolog III (2-2) of Jobin Yvon spectrometer in the S/R mode.

Kinetic experiments were carried out by mixing a P103 (20 g/L) containing $PyC_{18}$ with a probe-free P103 solution (at different concentrations) in a 2 mm thick cell. The ratio of P103 containing $PyC_{18}$ to the probe-free P103 was 1/20. All the measurements were carried out at 25 °C. The excitation wavelength was 344 nm, and the emission was monitored every 30 s at $\lambda_{em}$ = 480 nm for the excimer and $\lambda_{em}$ = 375.5 nm for the monomer.

At 25 °C, the P103 form micelles above the critical micelle concentration (cmc = 0.7 g/L)[13] with a hydrodynamic radius $R_h$ = 8 nm[14] and an aggregation number $N_{agg}$ around 59.[15] When the P103 solution is heated above the cloud point and cooled down to room temperature, the micelles dissolve randomly the hydrophobic probe $PyC_{18}$. In Figure 1 we present

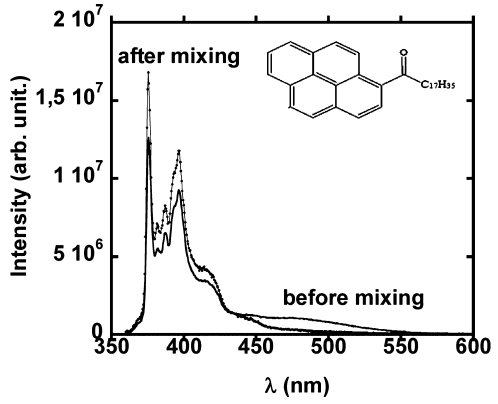


**Figure 1.** Emission spectra ($\lambda_{ex}$ = 344 nm) of $PyC_{18}$ in aqueous solution of P103 micelles. The spectrum labeled "before mixing" refers to a solution of P103 20g/L containing PyC18. The spectrum "after mixing" refers to the solution obtained by mixing 0.05 mL of the full micelles with 1 mL of empty P103 micelles (20 g/L). Inset: molecular structure of the probe $PyC_{18}$.

the fluorescence spectrum of P103 (20g/L) micelles containing $PyC_{18}$. The spectrum has a broad excimer emission with a peak at 480 nm and monomer fluorescence at 375.5−400 nm. The existence of the excimer emission at 480 nm infers the presence of micelles bearing two or more $PyC_{18}$ molecules. When the P103 20 g/L with $PyC_{18}$ is mixed with an excess $PyC_{18}$-free P103 solution, the spectrum evolves and shows a higher monomer emission and no discernible excimer band, which infers the distribution of $PyC_{18}$ among all the micelles yielding only micelles with one probe. The ratio of excimer-to-monomer intensities ($I_E/I_M$) increases linearly with increasing the average number of probes per micelle $\langle n \rangle$ (not shown here): $\langle n \rangle$ = [$PyC_{18}$]/([P103] − cmc). This infers that $PyC_{18}$ undergo a random Poisson distribution among the P103 micelles up to $\langle n \rangle \approx 3$.[16]

In Figure 2, we show the result of a time-scan experiment in which we monitor the decrease in the excimer intensity ($\lambda_{em}$ =

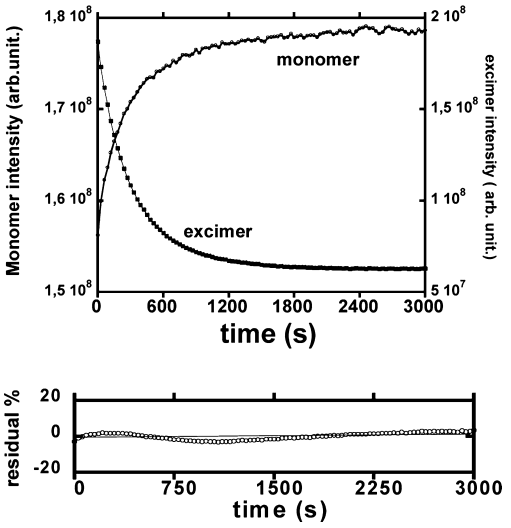


**Figure 2.** Time-scan experiment monitoring the decrease in the excimer emission ($\lambda_{em}$ = 480 nm) and the increase of the monomer emission ($\lambda_{em}$ = 375.5 nm) after mixing 1 mL of a P103 solution (20 g/L) with 0.05 mL of P103 solution (20 g/L) containing $PyC_{18}$. The solid line represents the fit to a single-exponential expression. Inset: residuals from the exponential fit of the excimer decay.

480 nm, $I_E$) and the increase of the monomer intensity ($\lambda_{em}$ = 375.5 nm, $I_M$) following the mixing of P103 (20 g/L) containing $PyC_{18}$ with P103 solution at 20g/L. Particularly for the case of small $\langle n \rangle$ ($\langle n \rangle$ < 0.5) the $I_E$ and $I_M$ are proportional to the fraction of micelles bearing two probes $I_E \propto P(t)$ and $I_M \propto P(t)$.[17] Unlike the probe exchange in common surfactant micelles (Triton X100), which shows rigorous single exponential behavior,[6] the $I_E$ and $I_M$ decays exhibit a small but noticeable deviation from the single exponential (Figure 2b). This is most likely due to the effect of polymer polydispersity on fusion and fragmentation.[2c] The relaxation time ($\tau$) from the single exponential is similar to the average value $\langle \tau \rangle$ calculated from the fit to two exponentials. When the kinetics is repeated at different copolymer concentration, we observe a strong dependence of the exchange rate $k_{decay} = 1/\tau$ on the concentration of empty micelles. In Figure 3 we show that $k_{decay}$ exhibits a linear dependence on the micelle concentration $k_{decay} = k_1 + k_2$[micelle], with [micelle] = ([P103] − cmc)/$N_{agg}$. The linear dependence of $k_{decay}$ vs [micelle] with a finite intercept reflects the existence of two mechanisms: a first-order process with a rate $k_1$ independent of the empty micelles ($k_1 = 1.07 \times 10^{-3}$ $s^{-1}$) and a second-order process with a linear dependence of $k_{decay}$ on [micelle] ($k_2$ = 25.5 $s^{-1}$ $M^{-1}$).

The exchange of solutes between micelles shares the same pathways with the exchange of copolymer chains (Chart 1). The transfer of a probe molecule (P) from a full to an empty micelle proceeds through three main paths (Chart 1): (a) one probe exits the full micelle to the aqueous phase and then enters an empty one, (b) the full micelles fragment into two micelles, each bearing one probe followed by the growth of the fragments via insertion of copolymer chains or fusion with an


dx.doi.org/10.1021/ma3018298 | Macromolecules XXXX, XXX, XXX−XXX

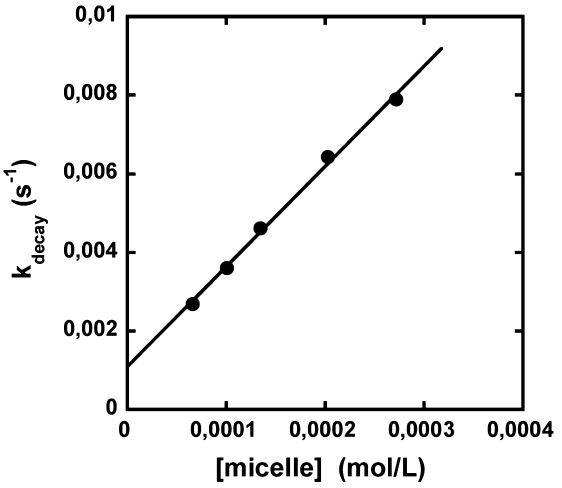


**Figure 3.** Relaxation rate $k_{decay}$ calculated from the fits of the exchange decays of $PyC_{18}$ in P103 to the single exponential, plotted against the concentration of empty micelle.

empty micelle, and (c) the full micelles can fuse with empty micelles to form large ones that break into two proper micelles containing each one probe. The exit−entry and fragmentation−growth are first-order processes, which should lead to a constant exchange rate $k_{exit}$ and $k_{fra}$, respectively. The fusion−fragmentation is a bimodal process, which leads to second-order kinetics. In the case where the concentration of empty micelles is much larger than the full ones, the fusion−fragmentation gives pseudo-first-order kinetics with a rate $k_{fus}$[micelle]. The exchange rate can be written as $k_{decay} = k_{exit} + k_{fra} + k_{fus}$[micelle]. One can also imagine other side processes that are not considered in this analysis such as fragmentation of a full micelle in two fragments followed by their fusion. Micelles can also collide, adhere, exchange their contents, and fragment without fusing.

The rate liming for the probe exit−entry is either the water solubility ($C_w$) or the diffusion through the core/corona. In the case, where water solubility is the dominant barrier, the exit rate can be estimated from partitioning equilibrium $k_{exit} = k_{entry}C_w/n_m$, where $n_m$ is the average number of probes per micelle at equilibrium. The diffusion through the viscous PPO core should give $k_{entry}$ smaller than the diffusion controlled rate in water ($k_{entry} < 3 \times 10^9$ $M^{-1}$ $s^{-1}$). Probe solubility in P103 micelle infers that $n_w > 1$. $C_w$ of $PyC_{18}$ is too small to be detected easily but can be estimated using the energy for the transfer of one methylene group from water to the micelles ($\Delta\mu_{CH_2}$), $\ln(C_w) = \ln(C_w^0) - N\Delta\mu_{CH_2}/RT$,[18] where $C_w^0$ can be taken as the water solubility of 1-acetylpyrene ($N = 2$) ($10^{-6}$ mol/L). The different literature values of $\Delta\mu_{CH_2}$ give $C_w \approx 4.3 \times 10^{-15}$ mol/L,[18] $C_w \approx 4.7 \times 10^{-17}$ mol/L,[19,20] and $C_w \approx 2.5 \times 10^{-16}$ mol/L.[21] Even if we omit the role of the core viscosity on $k_{entry}$ ($k_{entry} \approx 3 \times 10^9$ $M^{-1}$ $s^{-1}$) and we take $n_m = 1$, we find $k_{exit}$ $1.3 \times 10^{-5}$, $7.5 \times 10^{-6}$, and $1.4 \times 10^{-7}$ $s^{-1}$, which is 2−4 orders of magnitude lower than the measured exchange rate. Moreover, an upper limit for $k_{exit}$ can be estimated from the exchange of $PyC_{18}$ between spherical micelles of sodium dodecyl sulfate (SDS) because (i) fragmentation and fusion are extremely slow in SDS in the absence of added salt,[23] (ii) the exchange is dominated by water solubility,[23] and (iii) the exit rate in SDS is expected to be faster than in P103 since the SDS core is smaller and less viscous than PPO core.[15,22,23] When the exchange of $PyC_{18}$ is carried out in SDS in absence of salt, following the same procedure as in ref 23, we found the exchange rate to be negligible compared to that in P103, which suggests that $k_{exit}$ can be safely neglected in P103. One might imagine an alternative exit mechanism where the probe exit is assisted by chain expulsion ($k^-$). When the P103 solution containing $PyC_{18}$ is diluted below the cmc, the $PyC_{18}$ does not dissolve in the PPO of the free chains but rather forms large aggregates. This confirms that the PPO of the free chains cannot solubilize the $PyC_{18}$. This result rejects the model of probe exit assisted by chain expulsion. Therefore, the first-order process involves mainly the fragmentation−growth mechanism.

The energy barrier to fragmentation is estimated from the combination of surface tension energy and core elastic energy as $E_{fission} \sim (N_{PPO})^{2/3}(N_{agg})^{2/3}x^{2/3}$, where $N_{PPO}$ is the chain length of the PPO and $x = N_{agg}^1/N_{agg}$, with $N_{agg}^1$ is the size of the fragment.[7] This favors the expulsion rate of single chains $N_{agg}^1 = 1$.[7] In the case of P103, the fragmentation rate measured with $PyC_{18}$ is less than $10^{-6}$ the estimated value of the expulsion rate of single chains ($k^- \approx 2000$ $s^{-1}$),[24] $k_{fra}/k^- \approx 10^{-6}$. However this argument is not sufficient to exclude the contribution of the fission in copolymer dynamics. For example, even in a system of small nonionic surfactant like Triton X-100, where fusion fragmentation dominates several aspects of their dynamics, the $k_{fra}/k^-$ is similar to that reported here $k_{fra}/k^- = 5.5 \times 10^{-6}$.

The second-order process $k_2$ is likely to be dominated by fusion−fragmentation, which involves several steps: collision of a full and an empty micelle, adhesion of these micelles, fusion of the two micelles to form a large one, exchange of the solute within the large micelle, and fragmentation of the large micelle into two proper micelles containing one probe each. Because the diffusion-controlled rate is more than $10^9$ times the measured $k_2$, the fusion−fragmentation process cannot be dominated by the collision step. The second-order fusion rate is found to be 25.5 $s^{-1}$ $M^{-1}$. Because fusion can either yield solute exchange or not, $k_{fus} = 2k_2 = 51$ $s^{-1}$ $M^{-1}$. The linear increase of $k_{obs}$ vs [micelle] infers that fragmentation of the large aggregate $2N_{agg}$, resulting from the fragmentation of two micelles is much faster than $k_{fra}$ of proper micelles. This is expected since the energy resulting from the fission of micelles of size $2N_{agg}$ is negative.[8] If the fission rate of $2N_{agg}$ were similar to that of the proper micelle $N_{agg}$, the $k_{obs}$ will level off at high concentration. Thus, the measured $k_2$ describes the rate of fusion $k_{fus}$. It has been shown in Triton X-100 and synperonic surfactants that fusion rate is independent of the polarity of the probe,[6] which infers that the second-order fusion rate reflects the rate of fusion. The energy barrier to fusion is the coronal energy resulting from the steric repulsion or the elastic energy of the corona. In the case studied here of crew-cut micelle (short corona), the elastic energy barrier is described as $E_{fusion} \sim N_{PEO}^{2/3}/N_{PPO}(N_{agg})^2$.[7] The barrier energy to insertion is $E_{fusion} \sim N_{PEO}/(N_{PPO})^{-4/9}(N_{agg})^{2/9}$, which makes fusion less probable than insertion.[13] The measured fusion rate is found to be less than $10^{-6}$ times the expulsion rate ($k^+ \approx 5 \times 10^6$ $s^{-1}$ $M^{-1}$).[24] Yet the fusion process still controls several aspects of the P103 dynamic such as the sphere-to-rod transition.[11]

In this article we show that fusion and fragmentation take place between proper micelles at equilibrium in the triblock copolymer $PEO_{17}PPO_{60}PEO_{17}$with a rate $10^6$ slower than the rate of chain expulsion and insertion.


dx.doi.org/10.1021/ma3018298 | Macromolecules XXXX, XXX, XXX−XXX

## AUTHOR INFORMATION

**Corresponding Author**

*E-mail rharbi@ujf-grenoble.fr.

## ACKNOWLEDGMENTS

This work was supported by the joint program ECOS-Nord M05P02E, MO6-P03 of the ministry of research and education (France). We acknowledge Prof Armando Soltero for providing the copolymer. We acknowledge M. Karrouch, E. Fevre, F. Hugenel, and Dr. Hélène Galliard for their technical support.

## REFERENCES

(1) (a) Hamley, W. In *Block Copolymers in Solution*; Hamley, I. W., Ed.; John Wiley & Sons: San Francisco, 2005. (b) *Amphiphilic Block Copolymers: Self-Assembly and Applications*;Alexandridis, P., Lindmann, B., Eds.; Elsevier: Amsterdam, 2000.

(2) (a) Nicolai, T.; Colombani, O.; Chassenieux, C. *Soft Matter* **2010**, *6*, 3111. (b) Lund, R.; Willner, L.; Richter, D. *Macromolecules* **2006**, *39*, 4566. (c) Won, Y. Y.; Davis, H. T.; Bates, F. S. *Macromolecules* **2003**, *36*, 953−955. (d) Johnson, B. K.; Prud'homme, R. K. *Phys. Rev. Lett.* **2003**, *91*, 118302.

(3) (a) Aniansson, E. A. G.; Wall, S. N. *J. Phys. Chem.* **1974**, *78*, 1024; **1975**, *75*, 857. (b) Aniansson, E. A. G.; Wall, S. N.; Almgren, M.; Hoffmann, H.; Kielmann, H.; Ulbricht, W.; Zana, R.; Lang, J.; Tondre, C. *J. Phys. Chem.* **1976**, *80*, 905. (c) Wall, S. N.; Aniansson, E. A. *J. Phys. Chem.* **1980**, *84*, 727.

(4) (a) Kahlweit, M. *J. Colloid Interface Sci.* **1982**, *90*, 92. (b) Lessner, E.; Teubner, M.; Kahlweit, M. *J. Phys. Chem.* **1981**, *85*, 3167.

(5) Waton, G.; Michels, B.; Zana, R. *Macromolecules* **2000**, *34*, 907.

(6) (a) Rharbi, Y.; Li, M.; Winnik, M. A.; Hahn, K. G. *J. Am. Chem. Soc.* **2000**, *122*, 6242. (b) Rharbi, Y.; Winnik, M. A.; Hahn, K. G. *Langmuir* **1999**, *15*, 4697. (c) Rharbi, Y.; Bechthold, N.; Landfester, K.; Salzman, A.; Winnik, M. A. *Langmuir* **2003**, *19*, 10.

(7) Halperin, A.; Alexander, S. *Macromolecules* **1989**, *22*, 2403.

(8) Dormidontova, E. E. *Macromolecules* **1999**, *32*, 7630.

(9) Burke, S. E.; Eisenberg, A. *Langmuir* **2001**, *17*, 6714.

(10) Denkova, A. G.; Mendes, E.; Coppens, M.-O. *J. Phys. Chem. B* **2009**, *113*, 989.

(11) Landazuri, G.; Fernandez, V. V. A.; Soltero, J. F.; Rharbi, Y. *J. Phys. Chem. B* **2012**, *116*, 11720.

(12) *Friedel-Crafts and Related Reactions*; Olah, G., Ed.; Wiley-Interscience: New York, 1963; Vol. 3, p 78.

(13) Alexandridis, P.; Holzwarth, J. F.; Hatton, T. A. *Macromolecules* **1994**, *27*, 2414.

(14) Fernandez, V. V. A.; Soltero, J. F. A.; Puig, J. E.; Rharbi, Y. *J. Phys. Chem. B* **2009**, *113*, 3015.

(15) Kadam, Y.; Yerramilli, U.; Bahadur, A.; Bahadur, P. *Colloids Surf., B* **2011**, *83*, 49.

(16) Infelta, P. P.; Gratzel, M. *J. Chem. Phys.* **1979**, *70*, 179.

(17) Hilczer, M.; Barzykin, A. V.; Tachiya, M. *Langmuir* **2001**, *14*, 4196.

(18) Kozlov, M. Y.; Melik-Nubarov, N. S.; Batrakova, E. V.; Kabanov, A. V. *Macromolecules* **2000**, *33*, 3305−3313.

(19) Tolls, J.; van Dijk, J.; Verbruggen, E. J. M.; Hermens, J. L. M.; Loeprecht, B.; Schuurmann, G. *J. Phys. Chem. A* **2002**, *106*, 2760−2765.

(20) Ferguson, A. L.; Debenedetti, P. G.; Panagiotopoulos, A. Z. *J. Phys. Chem. B* **2009**, *113*, 6405−6414.

(21) Taisne, L.; Walstra, P.; Cabane, B. *J. Colloid Interface Sci.* **1996**, *184*, 378.

(22) Nivaggioli, T.; Tsao, B.; Alexandridis, P.; Hatton, T. *A. Langmuir* **1996**, *11*, 119.

(23) Rharbi, Y.; Winnik, M. A. *J. Phys. Chem. B* **2003**, *107*, 1491.

(24) $k^-$and $k^+$ are extrapolated from Figures 1 and 2 of the reference: Zana, R.; Marques, C.; Johner, A. *Adv. Colloid Interface Sci.* **2006**, *345*, 123−126.